Journal of Renewable Materials

Tech Science Press

DOI: 10.32604/jrm.2023.026060

check for updates

ARTICLE

Preparation and Characterization of Thermoplastic Starch from Sugar Palm *(Arenga pinnata)* by Extrusion Method

Muhammad Ghozali[1,2], Yenny Meliana[2], Widya Fatriasari[3], Petar Antov[4] and Mochamad Chalid[1,*]

[1]Departement of Metallurgy and Material, Universitas Indonesia, Depok, 16424, Indonesia

[2]Research Center for Chemistry, National Research and Innovation Agency (BRIN), Kawasan PUSPIPTEK Serpong, Tangerang Selatan, 15314, Indonesia

[3]Research Center for Biomass and Bioproducts, National Research and Innovation Agency (BRIN), Jl Raya Bogor KM 46 Cibinong, Bogor, 16911, Indonesia

[4]Faculty of Forest Industry, University of Forestry, Sofia, 1797, Bulgaria

[*]Corresponding Author: Mochamad Chalid. Email: m.chalid@ui.ac.id

Received: 12 August 2022 Accepted: 20 September 2022

ABSTRACT

Sugar palm *(Arenga pinnata)* starch is considered an important renewable, biodegradable, and eco-friendly polymer, which is derived from agricultural by-products and residues, with great potential for the development of biocomposite materials. This research was aimed at investigating the development of TPS biocomposites from *A. pinnata* palm starch using an extrusion process. Palm starch, glycerol, and stearic acid were extruded in a twin-screw extruder. Scanning electron microscopy (SEM) analysis of TPS showed that the starch granules were damaged and gelatinized in the extrusion process. The density of TPS was 1.3695 g/mL, lower than that of palm starch, and the addition of stearic acid resulted in increased TPS density. X-ray diffraction (XRD) results showed that palm starch had a C-type pattern crystalline structure. The tensile strength, elongation at break, and modulus of elasticity of TPS were 7.19 MPa, 33.95%, and 0.56 GPa, respectively. The addition of stearic acid reduced the tensile strength, elongation at break and modulus of elasticity of TPS. The rheological properties, i.e., melt flow rate (MFR) and viscosity of TPS, were 7.13 g/10 min and 2482.19 Pa.s, respectively. The presence of stearic acid in TPS resulted in increased MFR and decreased viscosity values. The peak gelatinization temperature of *A. pinnata* palm starch was 70°C, while Tg of TPS was 65°C. The addition of stearic acid reduced the Tg of TPS. The thermogravimetric analysis (TGA) analysis showed that the addition of glycerol and stearic acid decreased the thermal stability, but extended the temperature range of thermal degradation. TPS derived from *A. pinnata* palm starch by extrusion method has the potential to be applied in industrial practice as a promising raw material for manufacturing bio-based packaging as a sustainable and green alternative to petroleum-based plastics.

KEYWORDS

Arenga pinnata; sugar palm starch; thermoplastic starch; glycerol; stearic acid; twin-screw extruder; biocomposites

1 Introduction

In recent years, bio-based materials have gained increased research and industrial interest as eco-friendly, sustainable, and renewable alternatives to conventional petroleum-based plastics [1]. Due to their

superior film-forming abilities and extensive use, starch-based biopolymers are one of the most promising alternatives [2]. Starch is a naturally occurring polymer having the benefits of being abundant, renewable, biodegradable, and relatively inexpensive. It has many applications, including food processing, paper production, pharmaceuticals, adhesives, formaldehyde scavenger, etc. [3–5]. In addition, starch has attracted considerable interest as a natural and renewable feedstock for manufacturing sustainable, biodegradable plastic products. However, starch is not a real thermoplastic; it cannot be employed directly in the majority of bioplastic applications due to its inherent properties. Typically, starch needs to be altered or combined with other substances to produce a more accurate balance of qualities [6–9]. To be used as a thermoplastic material, starch requires additional additives, with the main additive needed being a plasticizer [10,11]. Plasticizers are the most important materials that can increase the flexibility and processibility of thermoplastic starch (TPS) [12] by decreasing the intermolecular pressure and improving polymer chain mobility. Significant research has been implemented on the plasticization of TPS using glycerol, urea, formamide, isosorbide, dimethyl sulfoxide, and low molecular weight sugars [13–15]. Glycerol is the most widely used plasticizer for starch-based polymers [2,8,16].

In the presence of a plasticizer, starch can be converted into thermoplastic material utilizing solvent casting and extrusion methods [17]. The thermal extrusion method is also one of the most popular methods for manufacturing starch-based polymers [18]. In the presence of plasticizers, starch can be converted into thermoplastic polymers utilizing a traditional thermomechanical process that involves heating and shearing by extrusion. Since no hazardous waste is produced, this method is considered a scalable and ecologically friendly surface alteration method [19]. In addition, the extrusion method can also be carried out continuously and readily applied in industrial practice. The development of TPS utilizing a twin-screw extruder has been extensively studied and reported in the literature [20–24]. Furthermore, TPS can also be obtained using a single-screw extruder with a temperature ranging from 110°C to 140°C [8,10].

Bioplastic preparation using the extrusion method usually requires additives to facilitate the process, especially to reduce friction between the material to be extruded and the barrel wall, facilitate the flow of material in the extruder, and avoid sticking the material to the extruder barrel wall. Several studies on bioplastic preparation were carried out by adding stearic acid as a lubricant [25–30]. Different types of starch have been utilized as raw materials in the production of bioplastics such as corn starch [2,8,17,21,26,28,30–35], softwood flour [25], potato starch [16], rice starch [36], tapioca or cassava starch [22–24,27,29,37,38]. Among the above types of starch, only cassava starch biopolymer has been used as a raw material on an industrial scale. However, the use of tapioca starch will certainly intersect with food needs. Therefore, other starch sources are needed in order to dissolve the debate and criticism regarding the use of food sources as polymeric matrix [39]. Sugar palm (*Arenga pinnata*) starch, derived from agroindustrial by-products and residues [40], represents a natural biopolymer and a promising renewable alternative to petroleum-based materials for manufacturing packaging films [41]. Sugar palm starch can be extracted from the *A. pinnata* stem when it no longer produces sugar and fruits [39,42]. The starch content of sugar palms ranges from 10.5%–36.7% [43]. Several studies have used sugar palm starch as a bio-based raw material to manufacture TPS [12,39,40,42,44]. The preparation of TPS from sugar palm starch using the solution casting method was reported by several authors [12,40,45]. Ilyas et al. [40] reported density, tensile strength, and elongation at break values of the TPS films of 1.413 g/mL, 4.8 MPa, and 38.10%, respectively. Other authors reported a density value of TPS of 1.40 g/mL [12] and tensile strength and elongation at break of the TPS films of 2.42 MPa and 8.03%, respectively [12].

To the best of our knowledge, there is limited literature reporting the use of palm starch from *A. pinnata* as a raw material for TPS bioplastic preparation by a twin-screw extruder. The aim of this research work was to utilize and investigate the development of TPS using sugar palm (*A. pinnata)* starch as a potential raw

material with glycerol and stearic acid as additives using a twin-screw extruder and evaluate their chemical structure, physical, mechanical, rheological, and thermal properties.

2 Material and Methods

2.1 Materials

Arenga pinnata palm starch was obtained from the local industry with an amylose content of 23.19%. Glycerol (CAS: 56-61-5) and stearic acid (CAS: 57-11-4) were purchased from Merck, Darmstadt, Germany.

2.2 Preparation of Thermoplastic Starch (TPS)

Thermoplastic starch (TPS) was prepared using a twin-screw extruder. Sugar palm starch (70%w), glycerol (30%w), and stearic acid (1 phr of the weight of palm starch + glycerol) were mixed and stirred first using a mixer until evenly distributed at room temperature. The mixture of palm starch, glycerol, and stearic acid was then stored in a closed container for one night to diffuse the glycerol into the palm starch granules completely. Furthermore, the extrusion process of a mixture of palm starch, glycerol stearic acid was carried out using a twin-screw extruder (Compounder ZK 16 T × 36L/D, Collin, Germany) with a screw speed of 90 rpm and a barrel temperature of 40°C/80°C/120°C/150°C/150°C/150°C/150°C/150°C in zones 1–8. Stearic acid was used as a lubricant to prevent the material from sticking to the screw and clogging the output end of the screw [25–30]. The mixture of palm starch and glycerol was named TPS, while the mixture of palm starch, glycerol, and stearic acid was labeled as TPSS. The resulting TPS and TPSS pellets were then stored in closed containers for analysis. The process of preparation of TPS is shown in Fig. 1.

Figure 1: Preparation of TPS composites

2.3 Fourier Transform Infrared (FTIR) Analysis

Fourier-Transform Infrared Spectroscopy (Bruker Tensor II, Germany) was used to examine the functional groups of the palm starch powder, TPS, and TPSS sheets. 32 scans were recorded for each sample while it was set in attenuated total reflectance (ATR) mode with a diamond ATR crystal at a wavenumber range between 500 and 4000 cm^{-1}.

2.4 Scanning Electron Microscopy (SEM) Analysis

The surface morphology of palm starch powder and the fractured surface morphology of TPS was examined using scanning electron microscopy (JEOL, JSM-IT200, Japan) at 3 kV for palm starch and 10 kV for TPS. Following submersion in liquid nitrogen, the TPS sample was broken. The surfaces had a thin gold layer applied to them before analysis.

2.5 X-Ray Diffraction (XRD) Analysis

Malvern Panalytical's XRD Aeris Ultrafast detector pixel 1D was used for the X-ray diffraction measurements. The X-ray diffraction pattern observed the 1.54 wavelength, 40 kV voltage, and 15 mA filament emission. The radiation reflection of palm starch powder, TPS, and TPSS film were measured at

the 2θ angle of 5°–50°. Furthermore, the percentage crystallinity (% crystalline) of palm starch, TPS, and TPSS samples were calculated as follows [46]:

$$X_c = \frac{I_{002}}{I_{002} + I_{am}} \times 100 \quad (1)$$

where I_{002} is the maximum intensity of diffraction of the (002) between 2θ of 22° to 23° and I_{am} is the intensity minimum of an amorphous region between 2θ 18° to 19°.

2.6 Mechanical Properties Analysis

Tensile tests using an electronic universal testing machine (UTM) (Shimadzu AG-X plus 50 kN, Japan), in accordance with ASTM D 638-14 standard [47], type V specimens at 21°C and relative humidity of around 50% were used to determine the mechanical properties of the TPS and TPSS films. Five specimens of each TPS and TPSS film type were evaluated at tensile rates of 10 mm/min. Each sample was randomly measured three times at various locations using a digital thickness gauge (Preisser Digi-met, Germany) to determine the film thickness.

2.7 Rheological Properties

The rheological properties of TPS and TPSS bioplastics were analyzed using the Melt Flow Index (MFI). Measurement of melt flow rate (MFR), viscosity, and shear rate value was carried out at 190°C.

2.8 Differential Scanning Calorimeter (DSC) Analysis

The DSC measurements were carried out with a Perkin Elmer DSC 4000, USA. DSC analysis was carried out with approximately 5 mg palm starch powder, TPS, and TPSS samples on a standard aluminum pan to determine the samples' glass transition temperature (Tg). Each sample was heated until 200°C with a 10 °C/min heating rate under a nitrogen atmosphere (flowrate = 20 mL/min).

2.9 Thermogravimetric Analysis (TGA) Analysis

The thermal stability of TPS, TPSS, and palm starch powder was evaluated using a thermogravimetric analyzer (TGA 4000, Perkin Elmer, USA). A crucible pan containing 5 mg of sample was heated from 25°C to 600°C at a rate of 10 °C/min. A 20 mL/min flow was used to purge the nitrogen gas.

3 Results and Discussion

3.1 Chemical Structure

Graphical representation of the chemical structure of palm starch, TPS, and TPSS by FTIR analysis is shown in Fig. 2. In general, the FTIR spectra of palm starch, TPS, and TPSS showed absorption peaks at similar wave numbers. The absorption peak widened at a wave number of about 3265 cm^{-1} associated with the hydroxyl group (-OH), while the absorption peak at a wave number of about 2921 and 2884 cm^{-1} was associated with the C-H stretching [12,40,42]. Additionally, the H-O-H vibration of water molecules causes the absorption peak at wave number 1645 cm^{-1} [12], while the absorption peak at wave number between 1200 and 900 cm^{-1} is the C-O, C-C, and C-O-H vibration [20].

The absorption peaks around 1330–1450 cm^{-1} are related to CH_2 bending and wagging (out of plane bending) of CH_2 [48]. The overlap of C-H stretching and O-H bending between 1500 and 1200 cm^{-1} makes it challenging to identify various absorption peaks in this spectrum [17]. Similar absorption peaks of palm starch were also reported by previous studies [12,40,42], while the FTIR result of TPS was verified by Sahari [12] and Ilyas et al. [40].

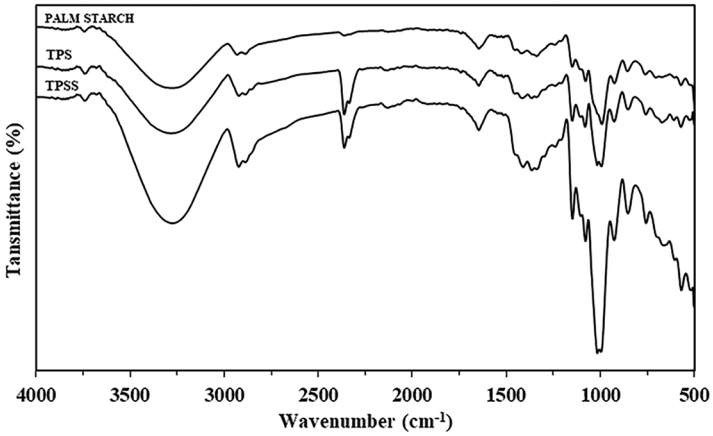

Figure 2: FTIR Spectrum of palm starch, TPS, and TPSS

3.2 Physical Properties

The density was measured (five replicates) in accordance with the ASTM D 792 standard [49] at 23°C and 50% relative humidity. A graphical representation of the density of palm starch, TPS, and TPSS is shown in Fig. 3.

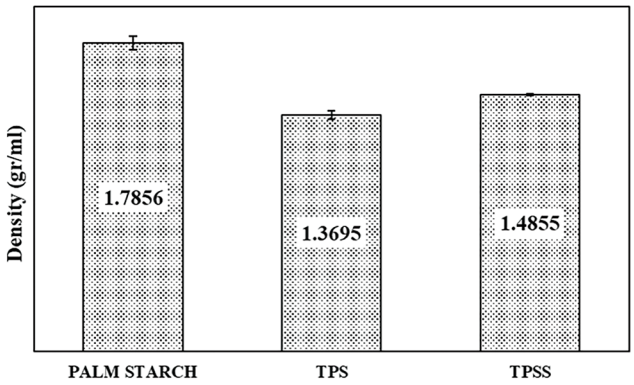

Figure 3: The density of palm starch, TPS, and TPSS

The determined density values of palm starch, TPS, and TPSS were 1.7856, 1.3695, and 1.4855 g/mL, respectively. This revealed that the presence of glycerol as a plasticizer decreased TPS density [39,45]. The presence of plasticizer reduces and weakens internal hydrogen bonding between starch molecules while increasing intermolecular spacing [39], thereby increasing the free volume and decreasing the density of TPS. Previous solvent casting methods reported that TPS's density values varied from 1.40 [45] to 1.413 g/mL [40]. The density value of TPS obtained in this research was lower, which proved that using the extrusion method to prepare TPS could further increase the interaction between the plasticizer and palm starch, leading to increased free volume and lower density. The addition of glycerol and stearic acid also reduced the density of TPS bioplastics. However, the TPSS density value was higher than the TPS density value. Stearic acid as a lubricant prevents the material from sticking to the screw [10,13,16,18–20], which facilitates the flow and reduces the interaction time between starch and plasticizer, resulting in a lower free volume of TPSS compared with TPS. According to La Fuente et al. [20], the extrusion technique favors chain alignment concerning the flow direction, producing materials with more cleanly and consistently ordered molecules [20]. These neatly arranged molecules result in a higher density value

of TPSS than TPS. This phenomenon of lower TPS density compared to *A. pinnata* palm starch was also confirmed by percentage crystallinity (% crystalline) in the XRD analysis.

3.3 Morphological Observation

Surface morphology of palm starch and cross-section morphology of TPS bioplastics were observed using SEM. The TPS sample was cut crosswise in liquid nitrogen prior to SEM testing. Fig. 4. shows the surface morphology of palm starch and the cross-section surface of TPS bioplastic. In Fig. 4, it can be seen that palm starch had a powder form and inhomogeneous size. Different types of palm starch powder were spherical and oval in shape. Similar results on the morphology of palm starch were also reported by Zhang et al. [42].

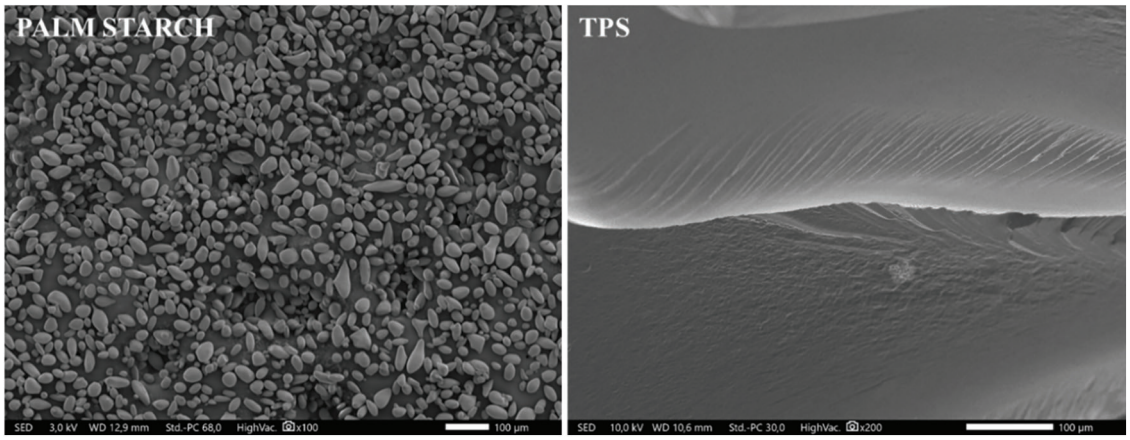

Figure 4: Surface and cross-section images of palm starch and TPS

The TPS cross-section surface appeared smooth, meaning the palm starch granules changed phase during processing in the extruder [20]. The palm starch granules melted or were physically broken into minute fragments as a result of the continual interaction between the heat, shear rate, and plasticizer in the extruder, which led to a smoother surface and loss of structure of the palm starch granules. No phase separation is seen in Fig. 4, indicating good compatibility. The smooth surface was caused by the addition of glycerol [12]. Glycerol is homogeneously incorporated within a network of hydrogen bonds of starch. Therefore, the morphology becomes more flexible, soft, and transparent [45]. When the glycerol and starch are mixed, hydrogen bonds weaken the interactions between starch molecules and increase the starch flowability. The relatively smooth cross-sections following glycerol extrusion showed that the starch granules exhibited significant deformation and fused together after extrusion under high temperatures and intense shearing. These outcomes also supported the superior processability of plasticized starch. The results are also consistent with the findings of Liu et al. [23], proving that the plasticization process of starch with glycerol in the extruder works well [23].

3.4 Crystallinity of Bioplastic Film

Semi-crystalline characteristics (the presence of crystalline and amorphous zones) of palm starch and bioplastics were observed using XRD. To examine the crystallinity of the bioplastic films, the XRD patterns of palm starch, TPS, and TPSS bioplastic films are displayed in Fig. 5. In Fig. 5, palm starch shows diffraction peaks with high intensity at 2θ of 15.1°, 17.2°, 18.0°, and 23.3°, which indicates that the characteristic palm starch has C-type pattern crystalline structure. The XRD result of palm starch was confirmed by previous studies [40,42,43]. After extrusion, the TPS diffraction pattern shows diffraction

peaks at 2θ of 11.9°; 13.3°, and 18.0°. The TPS diffraction pattern did not display any peaks of the C-type starch since the initial *A. pinnata* palm starch granules had been gelatinized during the thermoplasticization procedure in the twin-screw extruder. Meanwhile, the diffraction peak shown by TPSS bioplastic was 2θ of 13.4°, 17.2°, and 20.6° are the crystallinity characteristics of the V_H type. Ghambari et al. [33] reported that a broad hump diffraction peak pattern at 19° is a characteristic of completely amorphous materials [33]. However, TPS and TPSS showed a diffraction peak at 2θ of 19° with a bit of sharpness. This indicates that TPS and TPSS were not completely amorphous. This crystallinity is due to heat processing, which is caused by strong interactions between the hydroxyl groups of the starch molecular chain, which are then replaced by hydrogen bonds formed between the starch and the plasticizer. The initial crystals can cause them to be destroyed in the heat processing in the twin-screw extruder, but only a few crystals were formed in the heat processing [31]. This decrease in crystals formed was confirmed by percentage crystallinity (% crystalline). The double helix conformation is disrupted when gelatinizes starch, resulting in the amorphous zone. In contrast, recrystallization, which is aided by the development of microcrystalline connections, produces the crystalline region [20]. The presence of glycerol as a plasticizer increases the mobility of the molecular chains and causes crystallization [2]. The percentage crystallinity (% crystalline) of *A. pinnata* palm starch, TPS, and TPSS was 57.22%, 44.81%, and 47.74%, respectively. It can be seen that the percentage of crystallinity of TPS was lower than that of *A. pinnata* palm starch and TPSS. The lower percentage of crystallinity was since, in the twin-screw extruder, the initial crystals of *A. pinnata* palm starch were damaged by heat and shear, and only a few crystals were formed in the heat processing [31]. The percentage crystallinity (% crystalline) of *A. pinnata* palm starch >TPSS>TPS confirmed the strong relationship between the chemical and physical properties of *A. pinnata* palm starch, TPSS, and TPS, i.e., the higher percentage of crystallinity corresponded to higher density values of the material.

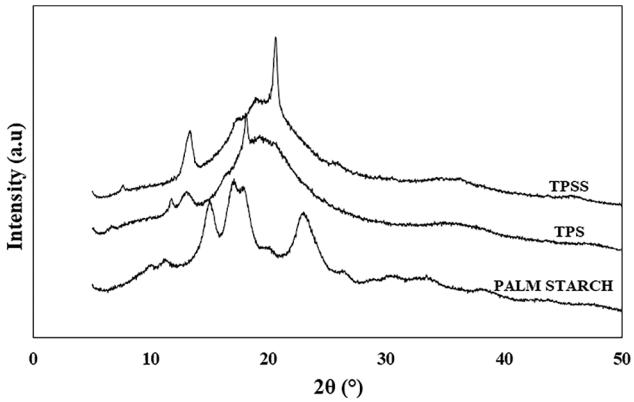

Figure 5: XRD Pattern of palm starch, TPS, and TPSS

Typically, the changes in the crystal structure of TPS can be attributed to amylose retrogradation or interactions between starch and plasticizing agents. The two primary components, amylose and amylopectin are embedded alternately in amorphous and crystalline lamellae seen in native starch granules. As previously stated, during the amylose processing of starch granules, the linear polymer dissociates out of the granules and crystallizes into numerous single helical crystal forms [33]. The extrusion process results in the breakdown of the original starch crystal structure, and then glycerol induces plasticization of the starch chain during extrusion and recrystallizes the starch [16]. The diffraction pattern of TPS and TPSS did not indicate the presence of a C-type pattern crystalline structure; this proved that the original *A. pinnata* palm starch granules had been gelatinized during the thermoplasticization process. These results are in accordance with the findings reported by Fourati et al.

[32], who used corn starch. Two contributions have been noted: (i) the B-type allomorph's diffraction peak would be at a 2θ of roughly 17°–18°. The presence of type B is anticipated given that type B develops during recrystallization (also known as retrogradation) of gelatinized starch at room temperature [50]; (ii) peaks between 13°C and 13.5°C and 19.8°C would be attributed to the V_H allomorph created by recrystallizing amylose with endogenous lipids found in corn starch [32].

3.5 Mechanical Properties

Fig. 6 displays the mechanical characteristics, including tensile strength, elongation at break, and modulus of elasticity.

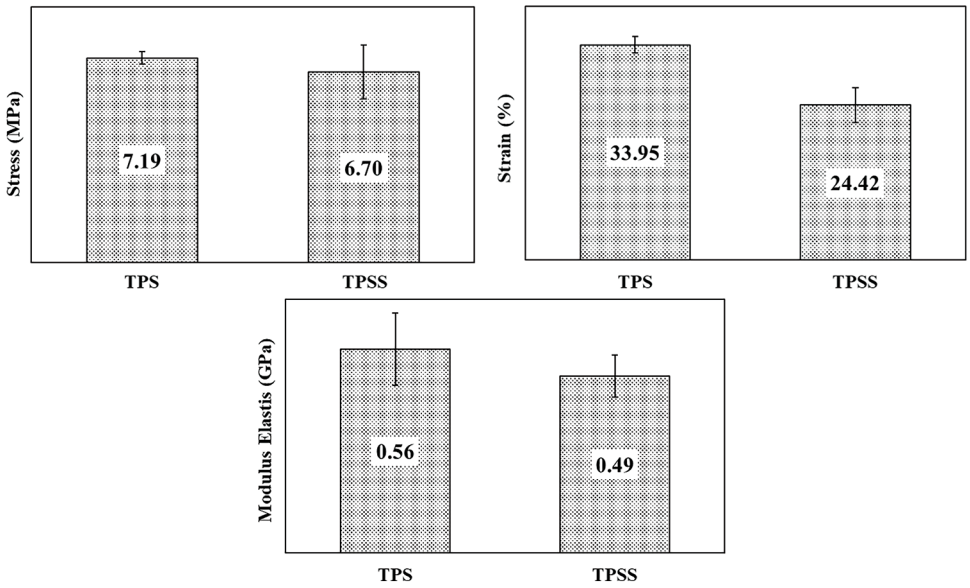

Figure 6: Mechanical properties of TPS and TPSS

TPS's tensile strength, elongation at break, and modulus of elasticity were 7.19 MPa, 33.95%, and 0.56 GPa, respectively. In a previous study of TPS preparation from palm sugar by solvent casting, Ilyas et al. reported the tensile strength and elongation at break of the TPS films from sugar palm starch of 4.8 MPa, and 38.10%, respectively [40], while Sahari [12] reported tensile strength and elongation at break of the TPS films of 2.42 MPa and 8.03%, respectively [12]. The tensile strength value of TPS obtained in this study was higher, which proved that the use of the extrusion method in the preparation of TPS could further increase the interaction between the plasticizer and palm starch compared to the solvent casting method. A strong correlation between the processing method applied and the mechanical properties of TPS was reported by Ilyas et al. [40]. The tensile strength, elongation at break, and modulus of elasticity values of TPSS were 6.70 MPa, 24.42%, and 0.49 GPa, respectively. Tensile strength, elongation at break, and modulus of elasticity values of TPSS were lower than TPS. This result showed that using stearic acid as a lubricant decreased the TPS bioplastic's mechanical properties. Stearic acid acts as a lubricant in the twin-screw extruder to prevent the material from sticking to the screw and clogging the output end of the screw [25–30]. The presence of stearic acid can reduce friction and facilitate the flow of material in the screw and barrel, which may lead to insufficient interaction time between starch and glycerol. This reduced or incomplete interaction of starch and glycerol may cause a lower value of the mechanical properties of TPSS compared to TPS. In the twin-screw extruder, the heat and shear of the extrusion process reduced the force between the starch molecules and disrupted the hard

structure. With more flexibility in the finished films, the extrusion method increased the plasticization of glycerol's effectiveness. The contents of starch, glycerol and stearic acid had a big impact on tensile strength and elongation at break. Plasticizing theory can be used to explain the relationship between starch and glycerol. The blocking effect refers to how the plasticizers weaken the link between the starch chains. Plasticizers typically work to inhibit molecules by interfering with their direct intermolecular interactions and expanding the space between the starch polymers [30].

3.6 Rheological Properties

A graphical representation of the melt flow rate (MFR), shear rate, and viscosity of TPS and TPSS is presented in Fig. 7. The obtained MFR values of TPS and TPSS were 7.13 and 8.89 g/10 min, respectively. Starch is not meltable and thus cannot be directly processed as a thermoplastic. In the extrusion process, starches are interrupted, and the crystalline structure order is disoriented due to the influence of glycerol, heat, and shear. The plasticization process allows its melt-processability and increases the flexibility and viscosity of TPS [12,39]. The addition of stearic acid as a lubricant in TPS increased the MFR value of TPSS. The increased MFR value was attributed to the presence of stearic acid as a lubricant which prevents the material from sticking to the screw [25], thereby reducing friction between the TPSS and the barrel wall. This reduced friction with the barrel wall results in decreased viscosity and an increased shear rate of TPSS. This phenomenon was evidenced by the decreasing value of TPS viscosity by 2482.19 to 1772.62 Pa.s at TPSS and increasing TPS shear rate by 9.61 to 11.05 s^{-1}.

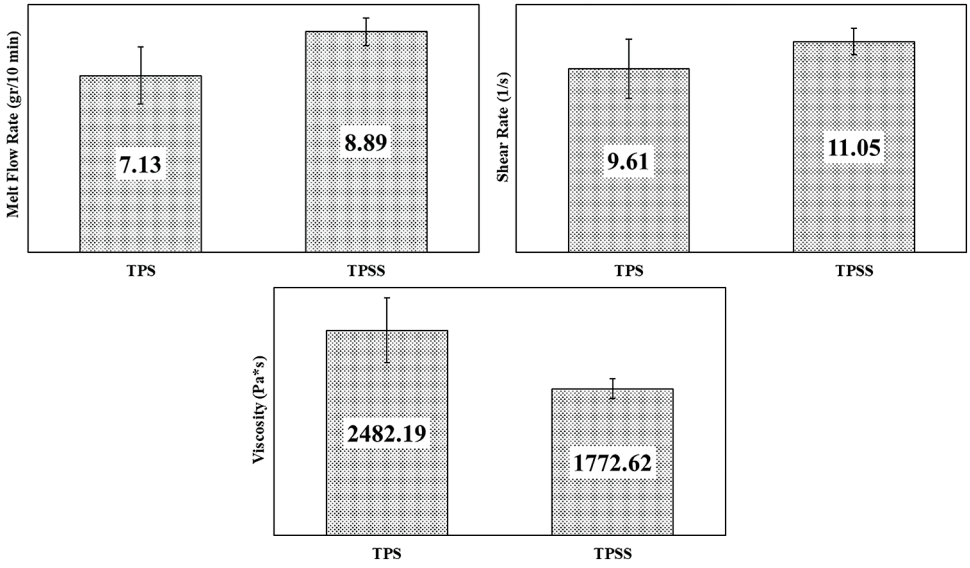

Figure 7: Melt flow rate, shear rate, and viscosity of TPS and TPSS

When plasticizers and starch are mixed together, hydrogen bonds are formed between starch and plasticizer, weakening the interactions between starch molecules, increasing the flowability of starch, and weakening the inter-and intra-molecular hydrogen bonds of starch [34]. The relationship between viscosity and shear rate was also revealed by Zhang et al. [34], i.e., decreased viscosity and increased temperature at a certain shear rate. As the temperature increases, the chain has greater energy; thus, the molecular energy of the chain increases, and the free volume of the molten liquid also increases. With increasing temperature, chain mobility increases, resulting in reduced flow resistance. The viscosity of each sample of TPS reduced as the shear rate was raised, demonstrating that the melt of the extruded

starch combination behaved like a pseudoplastic liquid. As shear rate increases, starch chain entanglement decreases, which weakens the inter- and intramolecular connections between starches and lowers flow resistance. Therefore, by accelerating shear and reducing viscosity, a compatible and evenly distributed combination can be identified [34].

3.7 Thermal Properties

The thermal properties of palm starch, TPS, and TPSS were studied by DSC analysis. A graphical representation of the DSC curve and the value of the glass transition temperature (Tg) of palm starch, TPS, and TPSS is presented in Fig. 8. It can be seen that the peak gelatinization temperature of palm starch was 70°C, very close to a previously reported peak temperature of gelatinization of palm starch of 67.7°C [43]. The gelatinization temperature of palm starch in this study was almost similar. However, it was lower than the results obtained by Zhang et al. [42], who reported that the gelatinization temperature of palm starch was around 98°C. In addition, Tg values of TPS and TPSS were 65°C and 50°C, respectively. The Tg value of TPS and TPSS was lower than the gelatinization temperature of palm starch. The decrease in the Tg value was attributed to the structure of the palm starch granules being damaged or destroyed by glycerol during the extrusion process at high temperatures [31]. Markedly, the plasticization process decreases the intermolecular forces between starch, increases free volume and, facilitates chain mobility, improves the flexibility of TPS, thus leading to the reduction of Tg [12]. Plasticization of starch by glycerol reduces and exchanges the inter- and intramolecular bonds between starch with a glycerol-starch hydrogen bond. Glycerol, as a plasticizer, effectively reduces internal hydrogen bonding while increasing intermolecular spacing, thereby decreasing Tg [39].

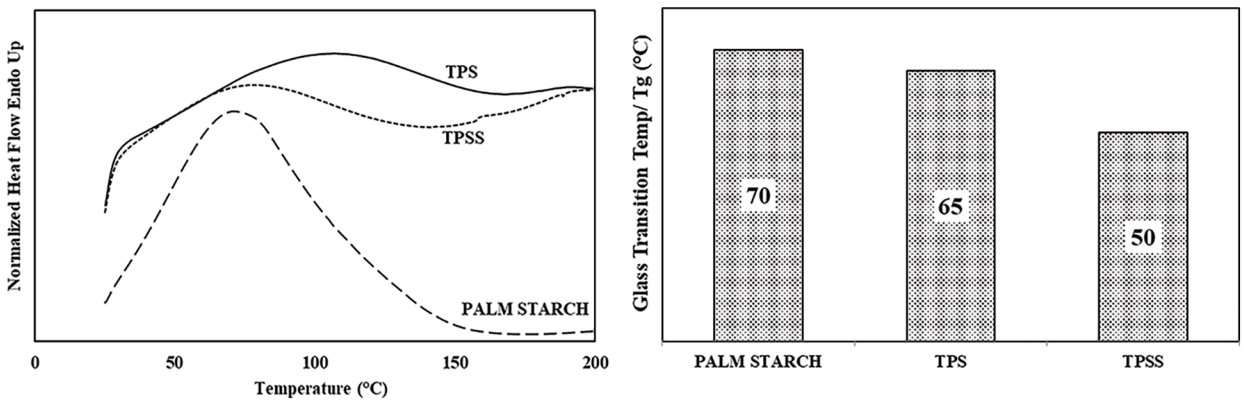

Figure 8: DSC curve and Tg value of palm starch, TPS, and TPSS

Thermal degradation and thermal resistance of palm starch, TPS, and TPSS, were studied by TGA analysis, and a graphical representation of the results is given in Fig. 9. Fig. 9 shows the thermal stability curves of palm starch, TPS, and TPSS. Palm starch exhibited two stages of thermal degradation. The initial stage of thermal degradation occurred at temperatures up to 150°C, with the peak of thermal degradation occurring at 70°C. This initial thermal degradation was related to the evaporation of water. A similar TGA pattern of palm starch was reported by Sahari et al. [12]. Thermal degradation in the second stage, namely the main thermal degradation, occurred in the temperature range of 260°C–400°C, with the peak of main thermal degradation occurring at 300°C. This main thermal degradation was also related to the dehydration of starch molecules to form glucose. Fig. 9 also shows that the final *A. pinnata* palm starch residue at 600°C was about 9% associated with the partial carbonization of starch. These results are similar to the previous study's findings [31].

Thermal degradation of TPS and TPSS was characterized by two stages in which the initial thermal degradation of TPS had a different pattern from that of palm starch. This initial thermal degradation was also related to the evaporation of water. The thermal degradation temperature range in the early stages was higher, compared to *A. pinnata* palm starch, up to 180°C, and the peak of thermal degradation in the early stages of TPS occurred at 150°C. At the same time, the main thermal degradation of TPS occurred in the temperature range of 260°C–400°C with two main stages. The first major thermal degradation was determined at a temperature of 260°C–310°C, with a peak of thermal degradation at 290°C associated with the decomposition of the glycerol-rich phase, while the second main thermal degradation occurred in the temperature range of 310°C–400°C with a peak thermal degradation at a temperature of 330°C, associated with the degradation of amylose and amylopectin starch [20–21,23]. The presence of glycerol caused the peak temperature of TPS thermal degradation to shift towards higher temperatures. This is because glycerol (plasticizer) in starch provides an advantage in thermal stability by increasing the mobility of molecular chains due to the plasticization process, thereby increasing the fluidity of the material and delaying the decomposition of the material caused by the process at high temperatures [23]. At 600°C, the TGA curve of palm starch showed better thermal resistance than TPS and TPSS. This was indicated by the amount of final residue of palm starch than TPS and TPSS. This lower thermal resistance of TPS and TPSS was associated with the decomposition of the glycerol-rich phase [20–21,23].

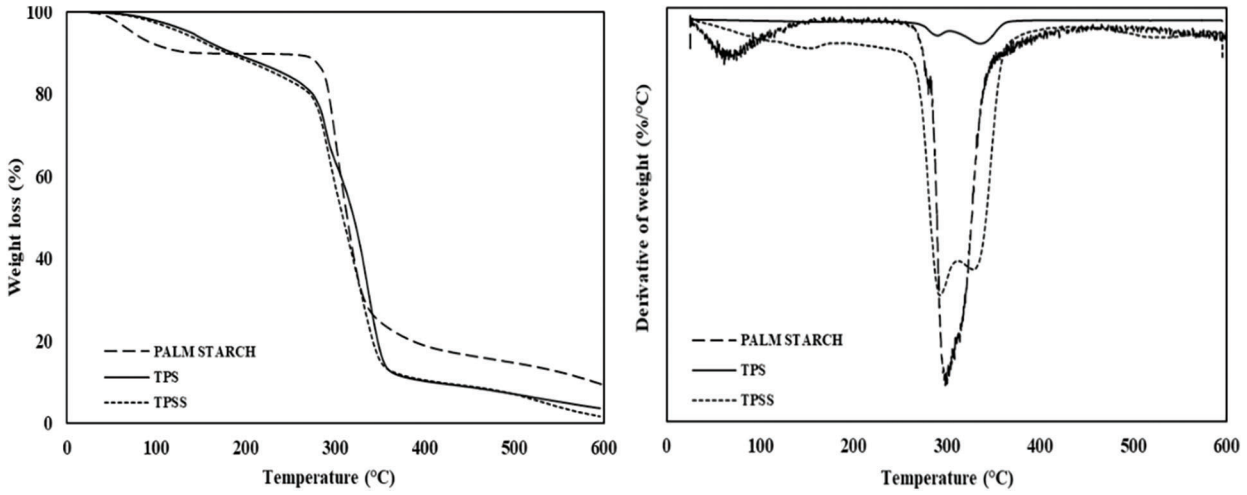

Figure 9: TGA and DTG Curve of palm starch, TPS, and TPSS

4 Conclusions

Thermoplastic starch (TPS) derived from sugar palm *(Arenga pinnata)* was successfully manufactured by an extrusion method using a twin-screw extruder. FTIR analysis showed that the absorption peaks of palm starch and TPS from *A. pinnata* were comparable to previously reported research. To note, the *A. pinnata* palm starch was characterized by a C-type pattern crystalline structure. The morphology of TPS showed that the starch granules were damaged and gelatinized in the extrusion process due to the presence of glycerol, heat, and shear. The resulting TPS had a lower density than *A. pinnata* palm starch, and the presence of stearic acid increased the density of TPS. The tensile, elongation at break, and modulus of elasticity of TPS was 7.19 MPa, 33.95%, and 0.56 GPa, respectively. The addition of stearic acid also reduced the tensile strength, elongation at break, and modulus of elasticity of TPS. The presence of stearic acid resulted in increased MFR and shear rate values but decreased the TPS viscosity. The peak gelatinization temperature of *A. pinnata* palm starch was 70°C, while Tg of TPS was 65°C. The addition of stearic acid resulted in reduced Tg of TPS. TGA analysis showed that adding glycerol and stearic acid

decreased the thermal stability but extended the temperature range of thermal degradation. Markedly, future research should focus on starch modification and optimization of the extrusion process to obtain TPS biocomposites with enhanced performance.

Acknowledgement: The authors are grateful for the research funding from The Hitachi Global Foundation Asia Innovation Award 2020. Also, the authors thank the facilities, scientific and technical support from Advanced Characterization Laboratories Serpong and Cibinong, National Research and Innovation Institute through E-Layanan Sains, Badan Riset dan Inovasi Nasional (BRIN).

Funding Statement: The authors received no specific funding for this study.

Conflicts of Interest: The authors declare they have no conflicts of interest to report regarding the present study.

References

1. Ghozali, M., Restu, W. K., Triwulandari, E., Anwar, M. (2020). Effect of metal oxide as antibacterial agent on thermoplastic starch/metal oxide biocomposites properties. *Polymer-Plastics Technology and Materials, 59(12),* 1317–1325. DOI 10.1080/25740881.2020.1738473.
2. Özeren, H. D., Olsson, R. T., Nilsson, F., Hedenqvist, M. S. (2020). Prediction of plasticization in a real biopolymer system (starch) using molecular dynamics simulations. *Materials & Design, 187,* 108387. DOI 10.1016/j.matdes.2019.108387.
3. Antov, P., Savov, V., Neykov, N. (2020). Sustainable bio-based adhesives for eco-friendly wood composites. A review. *Wood Research, 65(1),* 51–62. DOI 10.37763/wr.1336-4561/65.1.051062.
4. Gamage, A., Liyanapathiranage, A., Manamperi, A., Gunathilake, C., Mani, S. et al. (2022). Applications of starch biopolymers for a sustainable modern agriculture. *Sustainability, 14(10),* 6085. DOI 10.3390/su14106085.
5. Kristak, L., Antov, P., Bekhta, P., Lubis, M. A. R., Iswanto, A. H. et al. (2022). Recent progress in ultra-low formaldehyde emitting adhesive systems and formaldehyde scavengers in wood-based panels: A review. *Wood Material Science & Engineering,* 1–20. DOI 10.1080/17480272.2022.2056080.
6. Moad, G. (2011). Chemical modification of starch by reactive extrusion. *Progress in Polymer Science, 36(2),* 218–237. DOI 10.1016/j.progpolymsci.2010.11.002.
7. Belhassen, R., Vilaseca, F., Mutjé, P., Boufi, S. (2011). Preparation and properties of starch-based biopolymers modified with difunctional isocyanates. *BioResources, 6(1),* 81–102.
8. Alves, A., Grande, R., Carvalho, A. (2019). Thermal and mechanical properties of thermoplastic starch and poly (Vinyl alcohol-co-ethylene) blends. *Journal of Renewable Materials, 7,* 245–252. DOI 10.32604/jrm.2019.00833.
9. Zheng, Y., Xu, M., Tian, J., Yu, M., Tan, B. et al. (2022). Study on the properties of esterified corn starch/ Polylactide biodegradable blends. *Journal of Renewable Materials, 10(11),* 2949–2959. DOI 10.32604/ jrm.2022.019702.
10. Kundys, A., Ostrowska, J., Chojnacka, U., Grodzka, Z., Lange, A. et al. (2018). Enzymatic degradation of poly (butylenesuccinate)/thermoplastic starch blend. *Journal of Renewable Materials, 6,* 611–618. DOI 10.32604/ JRM.2018.00134.
11. Collazo-Bigliardi, S., Ortega-Toro, R., Chiralt, A. (2018). Reinforcement of thermoplastic starch films with cellulose fibres obtained from rice and coffee husks. *Journal of Renewable Materials, 6,* 599–610. DOI 10.32604/JRM.2018.00127.
12. Sahari, J., Sapuan, S. M., Zainudin, E. S., Maleque, M. A. (2013). Thermo-mechanical behaviors of thermoplastic starch derived from sugar palm tree (*Arenga pinnata*). *Carbohydrate Polymers, 92(2),* 1711–1716. DOI 10.1016/j. carbpol.2012.11.031.
13. López, O. V., Ninago, M. D., Lencina, M. M. S., García, M. A., Andreucetti, N. A. et al. (2015). Thermoplastic starch plasticized with alginate–glycerol mixtures: Melt-processing evaluation and film properties. *Carbohydrate Polymers, 126,* 83–90. DOI 10.1016/j.carbpol.2015.03.030.

14. Battegazzore, D., Bocchini, S., Nicola, G., Martini, E., Frache, A. (2015). Isosorbide, a green plasticizer for thermoplastic starch that does not retrogradate. *Carbohydrate Polymers, 119,* 78–84. DOI 10.1016/j.carbpol.2014.11.030.
15. Area, M. R., Montero, B., Rico, M., Barral, L., Bouza, R. et al. (2020). Properties and behavior under environmental factors of isosorbide-plasticized starch reinforced with microcrystalline cellulose biocomposites. *International Journal of Biological Macromolecules, 164,* 2028–2037. DOI 10.1016/j.ijbiomac.2020.08.075.
16. Nessi, V., Falourd, X., Maigret, J. E., Cahier, K., D'Orlando, A. et al. (2019). Cellulose nanocrystals-starch nanocomposites produced by extrusion: Structure and behavior in physiological conditions. *Carbohydrate Polymers, 225,* 115123. DOI 10.1016/j.carbpol.2019.115123.
17. Gilfillan, W. N., Moghaddam, L., Bartley, J., Doherty, W. O. S. (2016). Thermal extrusion of starch film with alcohol. *Journal of Food Engineering, 170,* 92–99. DOI 10.1016/j.jfoodeng.2015.09.023.
18. Vaidya, A. A., Gaugler, M., Smith, D. A. (2016). Green route to modification of wood waste, cellulose and hemicellulose using reactive extrusion. *Carbohydrate Polymers, 136,* 1238–1250. DOI 10.1016/j.carbpol.2015.10.033.
19. Gibril, M. E., Li, H., Li, X. D., Zhang, Y., Han, K. Q. et al. (2013). Reactive extrusion process for the preparation of a high concentration solution of cellulose in ionic liquid for in situ chemical modification. *RSC Advances, 3(4),* 1021–1024. DOI 10.1039/C2RA22296E.
20. La Fuente, C. I. A., do Val Siqueira, L., Augusto, P. E. D., Tadini, C. C. (2022). Casting and extrusion processes to produce bio-based plastics using cassava starch modified by the dry heat treatment (DHT). *Innovative Food Science & Emerging Technologies, 75,* 102906. DOI 10.1016/j.ifset.2021.102906.
21. Herniou-Julien, C., Mendieta, J. R., Gutiérrez, T. J. (2019). Characterization of biodegradable/non-compostable films made from cellulose acetate/corn starch blends processed under reactive extrusion conditions. *Food Hydrocolloids, 89,* 67–79. DOI 10.1016/j.foodhyd.2018.10.024.
22. Jariyasakoolroj, P., Supthanyakul, R., Laobuthee, A., Lertworasirikul, A., Yoksan, R. et al. (2021). Structure and properties of *in situ* reactive blend of polylactide and thermoplastic starch. *International Journal of Biological Macromolecules, 182,* 1238–1247. DOI 10.1016/j.ijbiomac.2021.05.024.
23. Liu, W., Wang, Z., Liu, J., Dai, B., Hu, S. et al. (2020). Preparation, reinforcement and properties of thermoplastic starch film by film blowing. *Food Hydrocolloids, 108,* 106006. DOI 10.1016/j.foodhyd.2020.106006.
24. Yusoff, N. H., Pal, K., Narayanan, T., de Souza, F. G. (2021). Recent trends on bioplastics synthesis and characterizations: Polylactic acid (PLA) incorporated with tapioca starch for packaging applications. *Journal of Molecular Structure, 1232,* 129954. DOI 10.1016/j.molstruc.2021.129954.
25. Hietala, M., Mathew, A. P., Oksman, K. (2013). Bionanocomposites of thermoplastic starch and cellulose nanofibers manufactured using twin-screw extrusion. *European Polymer Journal, 49(4),* 950–956. DOI 10.1016/j.eurpolymj.2012.10.016.
26. Lendvai, L., Karger-Kocsis, J., Kmetty, Á., Drakopoulos, S. X. (2016). Production and characterization of microfibrillated cellulose-reinforced thermoplastic starch composites. *Journal of Applied Polymer Science, 133(2)*. DOI 10.1002/app.42397.
27. Raabe, J., Fonseca, A. D. S., Bufalino, L., Ribeiro, C., Martins, M. A. et al. (2015). Biocomposite of cassava starch reinforced with cellulose pulp fibers modified with deposition of silica (SiO_2) nanoparticles. *Journal of Nanomaterials, 2015,* 493439. DOI 10.1155/2015/493439.
28. Teixeira, E., Lotti, C., Corrêa, A., Teodoro, K., Marconcini, J. et al. (2011). Thermoplastic corn starch reinforced with cotton cellulose nanofibers. *Journal of Applied Polymer Science, 120,* 2428–2433. DOI 10.1002/app.33447.
29. Teixeira, E. D. M., Curvelo, A. A. S., Corrêa, A. C., Marconcini, J. M., Glenn, G. M. et al. (2012). Properties of thermoplastic starch from cassava bagasse and cassava starch and their blends with poly (lactic acid). *Industrial Crops and Products, 37(1),* 61–68. DOI 10.1016/j.indcrop.2011.11.036.
30. Yan, Q., Hou, H., Guo, P., Dong, H. (2012). Effects of extrusion and glycerol content on properties of oxidized and acetylated corn starch-based films. *Carbohydrate Polymers, 87(1),* 707–712. DOI 10.1016/j.carbpol.2011.08.048.
31. Chen, J., Wang, X., Long, Z., Wang, S., Zhang, J. et al. (2020). Preparation and performance of thermoplastic starch and microcrystalline cellulose for packaging composites: Extrusion and hot pressing. *International Journal of Biological Macromolecules, 165,* 2295–2302. DOI 10.1016/j.ijbiomac.2020.10.117.

32. Fourati, Y., Magnin, A., Putaux, J. L., Boufi, S. (2020). One-step processing of plasticized starch/cellulose nanofibrils nanocomposites via twin-screw extrusion of starch and cellulose fibers. *Carbohydrate Polymers, 229,* 115554. DOI 10.1016/j.carbpol.2019.115554.
33. Ghanbari, A., Tabarsa, T., Ashori, A., Shakeri, A., Mashkour, M. (2018). Preparation and characterization of thermoplastic starch and cellulose nanofibers as green nanocomposites: Extrusion processing. *International Journal of Biological Macromolecules, 112,* 442–447. DOI 10.1016/j.ijbiomac.2018.02.007.
34. Zhang, Y. R., Wang, X. L., Zhao, G. M., Wang, Y. Z. (2013). Influence of oxidized starch on the properties of thermoplastic starch. *Carbohydrate Polymers, 96(1),* 358–364. DOI 10.1016/j.carbpol.2013.03.093.
35. Passaretti, M., Ninago, M., Paulo, C., Petit, H., Irassar, E. et al. (2019). Biocomposites based on thermoplastic starch and granite sand quarry waste. *Journal of Renewable Materials, 7,* 393–402. DOI 10.32604/jrm.2019.04281.
36. Shah, P., Prajapati, R., Singh, P. (2017). Enrichment of mechanical properties of biodegradable composites containing waste cellulose fiber and thermoplastic starch. *European Journal of Advances in Engineering and Technology, 4(4),* 282–286.
37. Kampangkaew, S., Thongpin, C., Santawtee, O. (2014). The synthesis of cellulose nanofibers from sesbania javanica for filler in thermoplastic starch. *Energy Procedia, 56,* 318–325. DOI 10.1016/j.egypro.2014.07.163.
38. Santos, L. C. G. D. S., Ayres, E., Padula, F. R. D. G. (2017). Tailoring the properties of thermoplastic starch with bamboo powder and/or hollow glass microspheres. *Journal of Renewable Materials, 5(3–4),* 307–312. DOI 10.7569/JRM.2017.634121.
39. Sanyang, M. L., Sapuan, S. M., Jawaid, M., Ishak, M. R., Sahari, J. (2016). Recent developments in sugar palm (*Arenga pinnata*) based biocomposites and their potential industrial applications: A review. *Renewable and Sustainable Energy Reviews, 54,* 533–549. DOI 10.1016/j.rser.2015.10.037.
40. Ilyas, R. A., Sapuan, S. M., Ibrahim, R., Abral, H., Ishak, M. R. et al. (2019). Effect of sugar palm nanofibrillated cellulose concentrations on morphological, mechanical and physical properties of biodegradable films based on agro-waste sugar palm (*Arenga pinnata* (Wurmb.) Merr) Starch. *Journal of Materials Research and Technology, 8(5),* 4819–4830. DOI 10.1016/j.jmrt.2019.08.028.
41. Asyraf, M. R. M., Rafidah, M., Ebadi, S., Azrina, A., Razman, M. R. (2022). Mechanical properties of sugar palm lignocellulosic fibre reinforced polymer composites: A review. *Cellulose, 29(12),* 6493–6516. DOI 10.1007/s10570-022-04695-3.
42. Zhang, L., Mei, J. Y., Ren, M. H., Fu, Z. (2020). Optimization of enzyme-assisted preparation and characterization of *Arenga pinnata* resistant starch. *Food Structure, 25,* 100149. DOI 10.1016/j.foostr.2020.100149.
43. Adawiyah, D. R., Sasaki, T., Kohyama, K. (2013). Characterization of arenga starch in comparison with sago starch. *Carbohydrate Polymers, 92(2),* 2306–2313. DOI 10.1016/j.carbpol.2012.12.014.
44. Ishak, M. R., Sapuan, S. M., Leman, Z., Rahman, M. Z., Anwar, U. M. et al. (2013). Sugar palm (*Arenga pinnata*): Its fibres, polymers and composites. *Carbohydr Polym, 91(2),* 699–710. DOI 10.1016/j.carbpol.2012.07.073.
45. Sahari, J., Sapuan, S. M., Zainudin, E. S., Maleque, M. A. (2012). A new approach to use *Arenga pinnata* as sustainable biopolymer: Effects of plasticizers on physical properties. *Procedia Chemistry, 4,* 254–259. DOI 10.1016/j.proche.2012.06.035.
46. Kiziltas, E., Kiziltas, A., Gardner, D. J. (2015). Synthesis of bacterial cellulose using hot water extracted wood sugars. *Carbohydrate Polymers, 124,* 131–138. DOI 10.1016/j.carbpol.2015.01.036.
47. ASTM (2014). ASTM D 638. *Standard Test Method for Tensile Properties of Plastics*. ASTM International, West Conshohocken, PA 19428-2959. USA.
48. Mano, J. F., Koniarova, D., Reis, R. L. (2003). Thermal properties of thermoplastic starch/synthetic polymer blends with potential biomedical applicability. *Journal of Materials Science: Materials in Medicine, 14(2),* 127–135.
49. ASTM (2000). ASTM D 792-20. *Standard Test Method for Density and Specific Gravity (Relative Density) of Plastics*. ASTM International, West Conshohocken, PA 19428-2959. USA.
50. Lourdin, D., Putaux, J. L., Potocki-Véronèse, G., Chevigny, C., Rolland-Sabaté, A. et al. (2015). Crystalline structure in starch. In: Nakamura, Y. (Ed.), *Starch: Metabolism and structure*, pp. 61–90. Tokyo, Japan: Springer.